



# NASF/AESF Foundation Research Reports



Project R-117 Q15

## Electrodeposition of Ni-Fe-Mo-W Alloys

15<sup>th</sup> Quarterly Report  
July-September 2016  
AESF Research Project #R-117

by  
*Yujia Zhang and Prof. E.J. Podlaha-Murphy\**  
Northeastern University  
Boston, Massachusetts, USA

### Introduction

Beginning in January 2013, the NASF, through the AESF Foundation Research Board, funded a three-year project on alloy plating at Northeastern University, in Boston, under the direction of Dr. Elizabeth Podlaha-Murphy, with emphasis on nickel-molybdenum-tungsten deposits. In 2016, a one-year extension was granted to examine the influence of oxide particulates codeposited with different combinations of Ni, Mo and W alloys on the resulting deposit composition in the generation of novel alloy composites. What follows is the third report on this new work.

In the last report, we examined the effect of titania particle concentration on Ni-W electrodeposition from an ammonia-free electrolyte with precise temperature control. With an increase in the electrolyte particle concentration, there was an associated higher deposit concentration. However, beyond an electrolyte particle concentration of 12.5 g/L, there was no further enhancement in the deposit particle content. A simple model following that of Guglielmi,<sup>1</sup> can capture this behavior.

Together with an increase in the amount of titania in the deposit, there was also a lower weight percentage of tungsten in the deposit. The decrease in the tungsten content was not due to a decrease in its deposition rate, or partial current density, but interestingly due to a larger nickel deposition rate. Furthermore, inspecting the polarization curves generated from the deposition electrolyte, and determining the side reaction partial current densities, suggested that the addition of the particle in a Ni-W-TiO<sub>2</sub> composite coating might be a better catalyst for hydrogen evolution compared to Ni-W alone, owing to the higher side reaction values when the particle was present.

In this report, pulse current (PC) electrodeposition was investigated to compare with direct current (DC) electrodeposition results on deposit composition and partial current density. The pulse frequency was varied to determine how it affected deposit composition and deposition rate.

Pulse current electrodeposition has several advantages over direct current electrodeposition, such as influencing adsorption and desorption phenomena. Significant grain refinement results from a larger instantaneous applied current density, and thus overpotential, when compared to an average, direct current value.<sup>2-3</sup>

Goldasteh and Rastegari<sup>4</sup> investigated PC deposition of Ni-W-TiO<sub>2</sub> composite coatings at a fixed cathodic current density of 100 mA/cm<sup>2</sup>, using a tungsten-rich, ammonium electrolyte at an elevated temperature of 75°C, with a cationic surfactant hexadecyltrimethylammonium bromide (CTAB). They found that the amounts of tungsten and TiO<sub>2</sub> in the PC plated coatings were slightly higher than those in DC plated coatings (2 wt% and 0.5 wt% higher for tungsten and TiO<sub>2</sub>, respectively) when the pulse frequency was 1000 Hz. They also reported that an increased pulse frequency corresponded with increased titania content in the deposit as well as reduced surface roughness.

---

\*Corresponding author:

Prof. E.J. Podlaha-Murphy  
Professor of Chemical Engineering  
Northeastern University  
Boston, Massachusetts 02115  
Phone: (617) 373-3796  
E-mail: e.podlaha-murphy@neu.edu

## Project R-117 Q15

Kumar, *et al.*<sup>5</sup> also compared PC and DC plated Ni-W-TiO<sub>2</sub> deposits at a fixed cathodic current density (150 mA/cm<sup>2</sup>), pulse frequency (14 Hz) and duty cycle (0.6), using an ammonia-containing a dimethyl sulfoxide (DMSO)-water electrolyte, which contained equal molar concentrations of nickel and tungsten, as well as a sodium lauryl sulfate (SLS) surfactant, and 0.6mM of the additive 2-butyne, 1,4-diol (BD) and at 70°C. A more uniform surface was observed for the PC plated deposits. Goldasteh<sup>4</sup> and Kumar<sup>5</sup> both obtained deposits with a low tungsten content (~25 wt%).

The influence of current density and the effect of pulse frequency on the Ni-W-TiO<sub>2</sub> composite coating composition, as well as the metal reaction rate have not yet been reported. In addition, composites with high tungsten content have not yet been examined.

Our goal for this report was to determine the effect of pulse frequency on the deposit composition, rate of metal reduction and morphology, using an ammonia-free electrolyte and with deposits having high tungsten content.

### Experimental

An ammonia-free electrolyte containing 0.15M nickel sulfate, 0.1M sodium tungstate, 0.285M sodium citrate, 1M boric acid was used as the plating electrolyte. The electrolyte pH was adjusted to a value of 8 with sodium hydroxide. Titanium dioxide microparticles (-325 mesh, Acros Organics) was then loaded to the electrolyte with a concentration of 12.5 g/L.

Electrodeposition was carried out on copper covered brass cylinder electrodes, having a diameter of 0.6 cm and length of 8 cm. A rotating Hull cell was used to quickly survey the different current density conditions. A plastic cylinder placed between the anode and the cathode was used to create the current distribution. The average applied pulse current density was -33 mA/cm<sup>2</sup> during the on-time ( $t_{on}$ ), and was zero during the off-time ( $t_{off}$ ). Pulse frequency was varied at 0.2 Hz, 2 Hz, 20 Hz and 200 Hz in this study, with a fixed duty cycle of 0.6. In all cases, the total on-time was 30 minutes. A double-jacked cell using a water bath was employed to maintain the electrolyte temperature at 25°C. Samples of direct current deposition were also prepared using the same experimental conditions (plating for 30 minutes at 25°C). A potentiostat (PINE Instrument Company, model AFCBP1), controlled by a function generator (AMEL, model AMEL 568) was used to generate the pulse current.

The composition and thickness were measured using x-ray fluorescence (XRF), (Kevex, model Omicron), in an air environment.

The morphology of the deposits was examined using scanning electron microscopy (SEM), (Hitachi, model 4800). SEM images were taken at a low current density region (~6-8 mA/cm<sup>2</sup>) and a high current density region (~50-80 mA/cm<sup>2</sup>). The rotating Hull cell electrode positions that corresponded to these regions were estimated by using a primary current distribution.

### Results

#### Composition

The rotating Hull cell provides a current distribution along the working electrode, as long as the current flow is governed by ohmic effects, described as a primary current distribution. In our previous study,<sup>6</sup> the Wagner number, a measure of kinetic to ohmic resistance, was determined to be 0.003 ( $\ll 1$ ), in a non-pulsing, DC situation, indicating that the current distribution was indeed nearly primary and that the local current density will change from a low to high value from end-to-end of the electrode. However, during pulse deposition the repetition of "on" and "off" times is expected to change the species' surface concentration which can then influence the reaction rate, and thus the kinetic resistance, which in turn affects the Wagner number in a dynamic way. Therefore, in this report, all data were plotted versus a dimensionless length  $L = x/h$  instead of an estimated local current density as done in our previous report,<sup>6</sup> with  $x$  being the distance from the low current density end of the working electrode and  $h$  being the total length of the working electrode.

Figure 1 compares the difference in deposit composition along the working electrode of the DC deposition deposits and the PC deposition deposits at different frequencies. Figure 1(a) shows that, for the DC condition, the tungsten content in the deposit increased from 45 to 55 wt% as the dimensionless cathode length  $L$  increased from 0.1 to 0.4, beyond which it remained almost constant. In cases corresponding to PC deposition, the amount of tungsten was consistently lower compared to DC deposition,

except at the very high current density end of the electrode where the tungsten content in the deposit was almost the same as in the DC case.

Figure 1(b) shows that with DC deposition, the particle content was constant (~4-5 %) over a large range of current densities. The deposit particle composition during PC deposition was similar to that for DC deposition at the very low and very high current density regions, but was slightly higher (~6-7 %) between these regions. As a result, PC deposition tended to increase slightly the amount of titania particles in the deposit at higher current densities, at the expense of lowering the amount of tungsten. This same observation was made in the previous report when the deposit was DC deposited, as noted above. With an increase in the particle electrolyte content and a subsequent increase in the deposit particle concentration, the tungsten content also decreased. Thus, the parameters that help the incorporation of the particles seem to hinder the tungsten deposition.

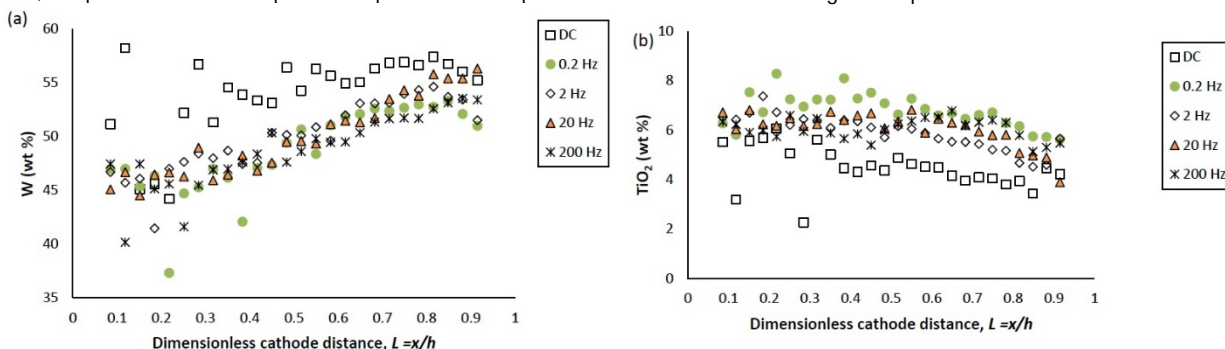
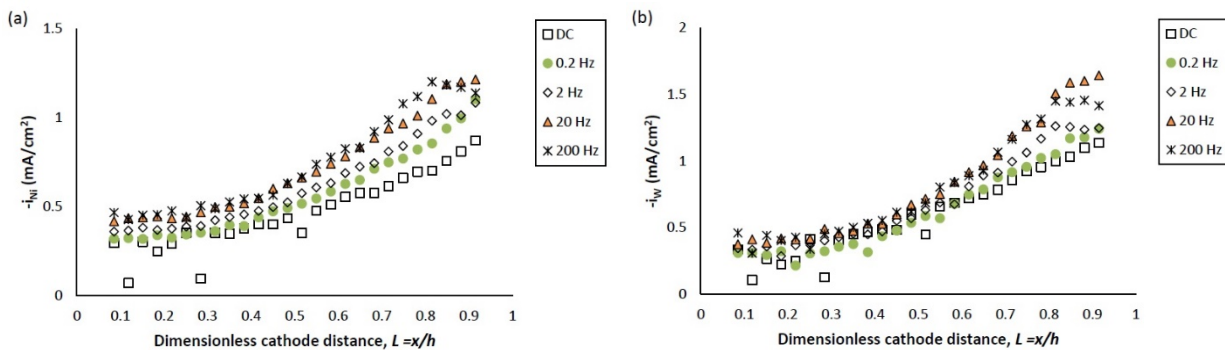


**Figure 1** - Ni-W-TiO<sub>2</sub> deposit composition of (a) tungsten and (b) TiO<sub>2</sub> (wt%) under DC and PC (with variable pulse frequency) conditions, with respect to a dimensionless length  $L$  representing lower and higher current densities with smaller and larger values, respectively.

In Figure 1, the weight percentages of (a) tungsten and (b) TiO<sub>2</sub> in the deposit, fabricated at variable pulse frequencies and a fixed duty cycle of 0.6 is also presented. The deposit composition was not largely influenced by the pulse frequency.

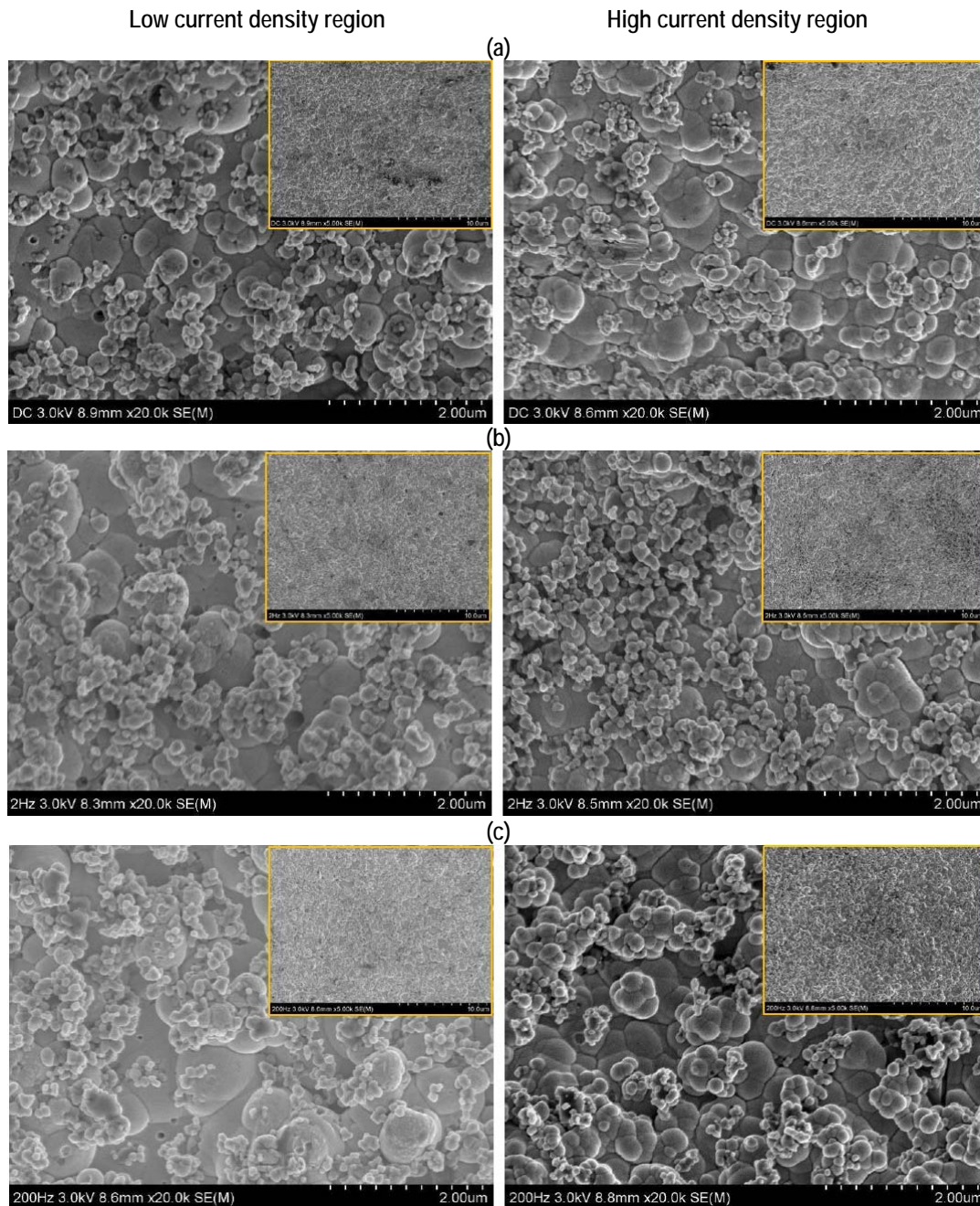
### Partial current density

Figure 2 shows the effect of PC deposition compared to DC deposition on the partial current densities of nickel and tungsten. Using the thickness measurement obtained by the XRF and applying a Faraday's law calculation, the partial current densities can be determined. The reaction rate of both nickel and tungsten deposition were enhanced over the entire length of the working electrode with PC deposition. Moreover, at the position where  $L < 0.8$ , the reduction of nickel (II) was enhanced more than that of tungsten (VI), leading to less tungsten in the deposit at the low current density end. At higher values of  $L$ , the enhancement of the nickel and tungsten reduction rate were almost equal, and thus there was no significant change of tungsten content, as was observed at the high current density end.



**Figure 2** - Partial current density of (a) nickel and (b) tungsten under DC and PC (with variable pulse frequency) condition, with respect to a dimensionless length  $L$  representing lower and higher current densities with smaller and larger values, respectively.

The effect of pulse frequency on the partial current of nickel and tungsten is also shown in Fig. 2. The reaction rate of nickel and tungsten were both enhanced as the pulse frequency was increased from 0.2 to 20 Hz, and remained almost unchanged with a further increase of pulse frequency to 200 Hz. Even though others in the literature used higher frequencies (up to 1000 Hz), in our case we expect that it would not have made a difference, as a limiting behavior was observed. Moreover, at the pulse frequency of 0.2 Hz, the reduction rate of both metal ions is very close to that of DC deposition, establishing the lower limit where surface species concentrations are essentially DC-like.



**Figure 3** - SEM images of Ni-W-TiO<sub>2</sub> deposits plated with (a) DC, (b) PC with the frequency of 2 Hz and (c) PC with the frequency of 200 Hz, in low current density (left) and high current density (right) regions, at low (5K, inset, upper right) and high (20K) magnifications.

### *Morphology*

The general appearance of the PC deposits had a dull, matte finish. Inspection of the microstructure by SEM is shown in Fig. 3 for (a) DC deposition, (b) PC deposition with a frequency of 2 Hz and (c) PC deposition with a frequency of 200 Hz (both with a duty cycle of 0.6), at low (5K) and high (20K) magnifications. Two regions on the working electrode were examined, at the low current density area with the value of  $L$  between 0.1 and 0.2, and the high current density region with the value of  $L$  between 0.8 and 0.9. The difference in the local current density between these regions is a factor of ten.

The SEM images show that PC deposition did not significantly change the morphology of the Ni-W-TiO<sub>2</sub> composite coatings. The deposits were all nodular, and the nodules were multiscale with more dendritic deposits occurring at higher current densities. Some nanoscale pits, were observed, particularly in the low current density region. Since the pit shapes were circular, they were perhaps due to the co-generation of evolving hydrogen from the side reaction.

Inspecting the high magnification images shows that the pit density and size became smaller with higher pulse frequency, suggesting that the pulsing deposition affects the hydrogen gas formation. With lower pulse frequency, however, no significant difference of pitting was observed. Interestingly, pitting was rarely observed in the high current density region where the rate of the hydrogen evolution side reaction was expected to be more vigorous.

The influence of pulse frequency affected two aspects: (1) it enhanced the metal partial current densities, particularly in the high current density regions, and (2) it changed the number and size of pits on the surface in the low current density region. We postulate that perhaps these two results are related through the adsorption of hydrogen, H<sub>ads</sub>. During the on-time, the adsorbed intermediate metal ion species are formed on the cathode surface, as well as adsorbed hydrogen. If the off-time facilitates the desorption of H<sub>ads</sub> from the electrode surface, thus more surface area is available for the reduction of metals, and their deposition rate goes up with pulsing. Thus, in the low current density region, there is still a large side reaction of hydrogen gas evolution, but the adsorption is lower. At the low current density end, the influence of pits from the gas bubble formation is evident, and the influence of adsorbed hydrogen on the metal reaction rate is less than at the high current density region.

### *Improving morphology with BD*

The additive, 2-butyne-1,4-diol (BD) in a nickel electrolyte under pulse deposition is known to promote grain refinement and result in a smoother morphology.<sup>7</sup> In a previous report, we have found that it improved the surface brightness of the Ni-W deposits.<sup>8</sup> Here, Ni-W-TiO<sub>2</sub> composites with the addition of 5 mM BD in the solution were deposited with a pulse frequency of 20 Hz and duty cycle of 0.6. The optical images (Fig. 4) show that in the presence of BD, the deposit became more reflective than the deposits from BD-free electrolytes under both DC and PC conditions. We are continuing work exploring this effect.



**Figure 4** - Photographs of Ni-W-TiO<sub>2</sub> composite coatings plated with DC with no BD, PC with no BD, PC with 5mM BD (from left to right) on the rotating Hull cell.

### **Conclusion**

Ni-W-TiO<sub>2</sub> composite coatings were electrodeposited under PC conditions at different pulse frequencies, and compared with DC condition deposits. With PC deposition, the deposit tungsten content was slightly decreased, with an increase in titania content. Interestingly, the tungsten deposition rate was not reduced. There was an enhancement of both nickel and tungsten partial current densities observed, particularly at high current densities, but the enhancement was larger for nickel compared to tungsten, resulting in more nickel in the deposit. PC deposition did not significantly alter the morphology of the deposit, but it did effect the pitting observed at low current densities. Initial studies combining the additive BD with PC deposition show a large improvement in surface appearance.

### References

1. N. Guglielmi, *J. Electrochem. Soc.*, **119** (8), 1009-1012 (1972).
2. M.S. Chandrasekar and M. Pushpavanam, *Electrochim. Acta*, **53** (8), 3313-3322 (2008).
3. N. Ibl, *Surface Technology*, **10** (2), 81-104 (1980).
4. H. Goldasteh and S. Rastegari, *Surf. Coat. Technol.*, **259** (Part C), 393-400 (2014).
5. K.A. Kumar, G.P. Kalaighan and V.S. Muralidharan, *Ceram. Int.*, **39** (3), 2827-2834 (2013).
6. Y. Zhang and E.J. Podlaha-Murphy, "Electrodeposition of Ni-Fe-Mo-W Alloys: Part 13," *Products Finishing*, (2016); <http://short.pfonline.com/NASF16Oct1>.
7. E.A. Pavlatou, M. Raptakis and N. Spyrellis, *Surf. Coat. Technol.*, **201** (8), 4571-4577 (2007).
8. A. Kola and E.J. Podlaha-Murphy, "Electrodeposition of Ni-Fe-Mo-W Alloys - Part 8," *Products Finishing* (2015); <http://short.pfonline.com/NASF15Jul1>.

### Past project reports

1. Quarter 1 (January-March 2013): Summary: *NASF Report in Products Finishing; NASF Surface Technology White Papers*, **78** (1), 11-17 (October 2013); <http://short.pfonline.com/NASF13Oct2>.
2. Quarter 2 (April-June 2013): Summary: *NASF Report in Products Finishing; NASF Surface Technology White Papers*, **78** (2), 18-27 (November 2013); <http://short.pfonline.com/NASF13Nov2>.
3. Quarter 3 (July-September 2013): Summary: *NASF Report in Products Finishing; NASF Surface Technology White Papers*, **78** (4), 11-16 (January 2014); <http://short.pfonline.com/NASF14Jan2>.
4. Quarters 4-6 (October 2013-June 2014): Summary: *NASF Report in Products Finishing; NASF Surface Technology White Papers*, **79** (2), 1-14 (November 2014); <http://short.pfonline.com/NASF14Nov1>.
5. Quarter 7 (July-September 2014): Summary: *NASF Report in Products Finishing; NASF Surface Technology White Papers*, **79** (7), 1-9 (April 2015); <http://short.pfonline.com/NASF15Apr1>.
6. Quarter 8 (October-December 2014): Summary: *NASF Report in Products Finishing; NASF Surface Technology White Papers*, **79** (10), 1-8 (July 2015); <http://short.pfonline.com/NASF15Jul1>.
7. Quarter 10 (April-June 2015): Summary: *NASF Report in Products Finishing; NASF Surface Technology White Papers*, **80** (7), 1-8 (April 2016); <http://short.pfonline.com/NASF16Apr1>.
8. Quarters 11-12 (July-December 2015): Summary: *NASF Report in Products Finishing; NASF Surface Technology White Papers*, **80** (12), 1-10 (September 2016); <http://short.pfonline.com/NASF16Sep1>.
9. Quarter 13 (January-March 2016): Summary: *NASF Report in Products Finishing; NASF Surface Technology White Papers*, **81** (1), 1-8 (October 2016); <http://short.pfonline.com/NASF16Oct1>.
10. Quarter 14 (April-June 2016): Summary: *NASF Report in Products Finishing; NASF Surface Technology White Papers*, **81** (3), 1-8 (December 2016); <http://short.pfonline.com/NASF16Dec1>.

### About the authors:



**Mr. Yujia Zhang** received his B.S. in Chemical Engineering at East China University of Science and Technology (ECUST) in 2007, and earned my M.S. in 2010. He worked in Houghton (Shanghai) Specialty Industrial Fluids Co., Ltd., a lubricant manufacturer, from 2010 to 2015 and is currently studying for his Ph.D. at Northeastern University.



**Dr. Elizabeth Podlaha-Murphy** is a Professor of Chemical Engineering at Northeastern University, Boston, MA. She has been active in electrodeposition for more than 20 years and currently leads efforts in the understanding of reaction mechanisms and kinetic-transport behavior governing electrodeposition. She received her Ph.D. in 1992 from Columbia University, New York, NY and a B.S./M.S. from the University of Connecticut, Storrs, CT.